RESEARCHERID
THOMSON REUTERS

[Obiad *et al.*, 6(1): January, 2019] ISSN 2349-0292
Impact Factor 3.802

GLOBAL JOURNAL OF ADVANCED ENGINEERING TECHNOLOGIES AND SCIENCES

INVESTIGATION OF OPTICAL, STRUCTURAL, MORPHOLOGICAL And THERMOELECTRIC PROPERTIES OF Ge DOPED NiO THIN FILMS

Saba A. Obiad[*1], Burak Y. Kadem[2] & Raheem G. Kadhim
[*1,2&3]Advanced Polymer lab, Physics department, Faculty of Science, University of Babylon, Iraq
DOI: 10.5281/zenodo.2536850

ABSTRACT

Nickel oxide thin films have been grown by reactive magnetron RF sputtering. The optical band gap has been estimated using Tauc equation and found to be decreased as the Ge dopant increase. The XRD results have suggested that the crystallinity of the NiO thin films has changed after doping with Ge, the (111) phase of NiO has disappeared after doping and another phase of NiO has exhibited (200) associated with Ge phase (220). This has suggested that the Ge dopants have sufficiently incorporated into the NiO lattice structure and changing the structure order and crystallinity. AFM and SEM have shown that surface morphology has changed after doping with Ge with rougher and grainier surface. EDX Analysis confirms the change in the lattice structure. The electrical conductivity has conducting a temperature dependency behavior. Seebeck coefficient has revealed that NiO thin film is a p-type semiconductor; while after doping it has changed to be n-type semiconductor as the Seebeck coefficient has become negative. Increasing the electrical conductivity without affecting the Seebeck coefficient has enhanced the power factor.

KEYWORDS: NiO thin film; Thermoelectric; Seebeck coefficient; Power factor..

INTRODUCTION

Nickel oxide (NiO) is considered as an attractive thin film due to its properties such as excellent chemical stability, electrical, optical and magnetic. NiO has been widely used in electrochromic display devices [1,2], antiferromagnetic material [3,4] and sensors [5,6]. NiO is usually considered as a p-type semiconductor films with a wide band-gap energy in the range from 3.6-4.0eV [7,8]. NiO thin films have been prepared using different physical and chemical techniques [9,10], among these several methods, reactive sputtering has been most widely used [11-13]. Thermoelectric power generators are based on Seebeck effect; this effect concerns the generation of the electromotive force (voltage) between the two ends of the thermoelectric device under a certain temperature difference. Once this device is connected to an electric circuit, the electric current flows through the circuit to generate electric power, and therefore heat can be converted into electricity [14]. Thermoelectric generators have the ability to convert the wasted heat into electrical energy without producing CO_2, toxic substances or other emissions [15]. Previously, the application of thermoelectric was based on bulk materials; however, by increasing combination of a higher heat flux with a higher package density in microelectronic devices, it is becoming more challenging to provide sufficient heat dissipation from the package [16]. As a result, thin film based thermoelectric devices are essential due to their properties such as efficient cooling capacity, small area and higher efficiency compared to devices made of bulk materials due to the stronger quantum confinement compared to that of bulk materials based thermoelectric devices [15-17]. The main challenge in improving the thermoelectric propertiesis that thethermoelectric parameters Seebeck coefficient (S), Electrical conductivity (σ) and thermal conductivity (k) are strongly interdependent [18]. Therefore, high thermoelectric performance could be obtained by decreasing the lattice thermal conductivityor increasing the power factor [18]. In the current study, the effects of adding Ge dopant to NiO thin films and their effects on the morphological, optical and thermoelectric properties have been investigated. Doping p-type NiO thin film with n-type semiconductor Ge, which is one of the group IV atoms, is expected to be harmless to the use of the oxide-based device [19]. The outcome of the thermoelectric is found to be effected by changing the thin film properties from p-type to n-type after doping. To the best of the authors' knowledge, this is the first attempt of doping NiO with Ge using reactive magnetron sputtering.

PREPARATION OF GERMANIUM DOPED NICKEL OXIDE

NiO thin Filmswere prepared using reactive magnetron sputteringon glass substrates [20]. The substrate was fixed at a distance of about 8mm from the target. The deposition was performed under vacuum pressure of 0.015mbar and substrate temperature of 300k for 20 minutes. The power of RF source was 150Watt. Doping of NiO by germanium (Ge)with different concentrations,1%,2% and 3% has been achieved under the same conditions. All the samples were subjected to heat treatment after the preparation at 625°C under vacuum.

RESULTS AND DISCUSSIONS

3.1 Optical properties

The optical properties of the studied thin films have been measured by Perkin–Elmer Lambda UV-visible spectrophotometer. NiO thin film is a p-type semiconductor with a direct band gap transition, a plot of the $\alpha h\upsilon^2$ versus the photon energy of the absorbed light gives the band gap [21-23]. The absorption coefficient (α) of NiO thin films has been estimated from the optical transmittance employing the following equation [24]:

$$\alpha = \frac{2.303}{d} \times \log(\frac{1}{T}) \quad (1)$$

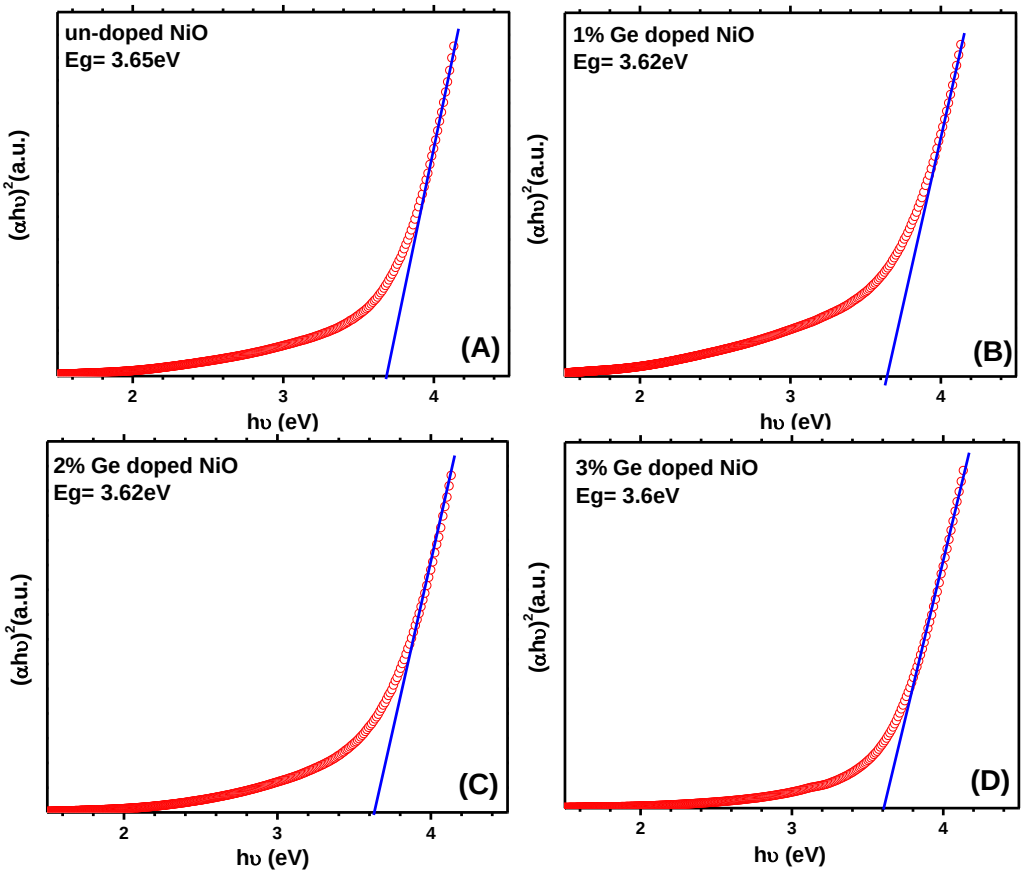

Fig.1: Tauc plot for energy band determination for the NiO thin films, (A) un-doped, (B) 1%Ge, (C) 2%Ge and (D) 3%Ge

where, T is the transmittance and d is the thickness of the NiO films. The absorption coefficient can also be used to determine the energy band gap (E_g) of the studied thin films using Tauc equation [25]:

$$\alpha h\nu = A(h\nu - E_g)^n \quad (2)$$

where, h is the Planck's constant, υ is frequency, A is constant and n is a value depends on the nature of transition. When n = 1/2 the band gap transition is allowed direct and the extrapolation of the linear region of $(\alpha h\upsilon)^2$ versus hυ curve provides the direct energy band gap [24]. The direct band gap for NiO-based thin films has shown an increase after the addition of Ge dopant. Fig.1A shows the estimation of the band gap for un-doped NiO thin film using Tauc plot, the resulted band gap (E_g) from this plot is about 3.65eV. The integration of 1%Ge (Fig.1B), 2%Ge (Fig.1C) and 3%Ge (Fig.1D) into the NiO thin films has resulted in slight decrease in E_g to 3.62eV, 3.62 and 3.6eV, respectively. This change could be attributed to the lattice constant change of NiO structure [19].

3.2 Morphological properties

The surface morphological propertiesof the deposited thin films were recorded using NanoSurf-AFM in contact mode as shown in Fig.2. The un-doped NiO thin films have exhibited uniformly distributed surface grains as

ISSN 2349-0292
Impact Factor 3.802

demonstrated in the AFM images. The grain size and the surface morphology have changed noticeablyafter doping with Ge dopant and with increasing the dopant concentration.

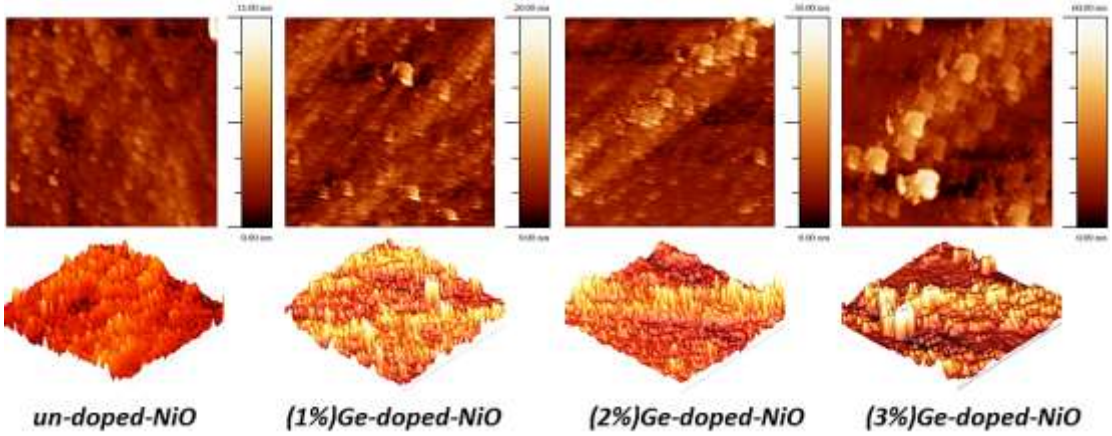

Fig.2: AFM characteristics for the NiO-based thin films with and without adding Ge at different concentrations

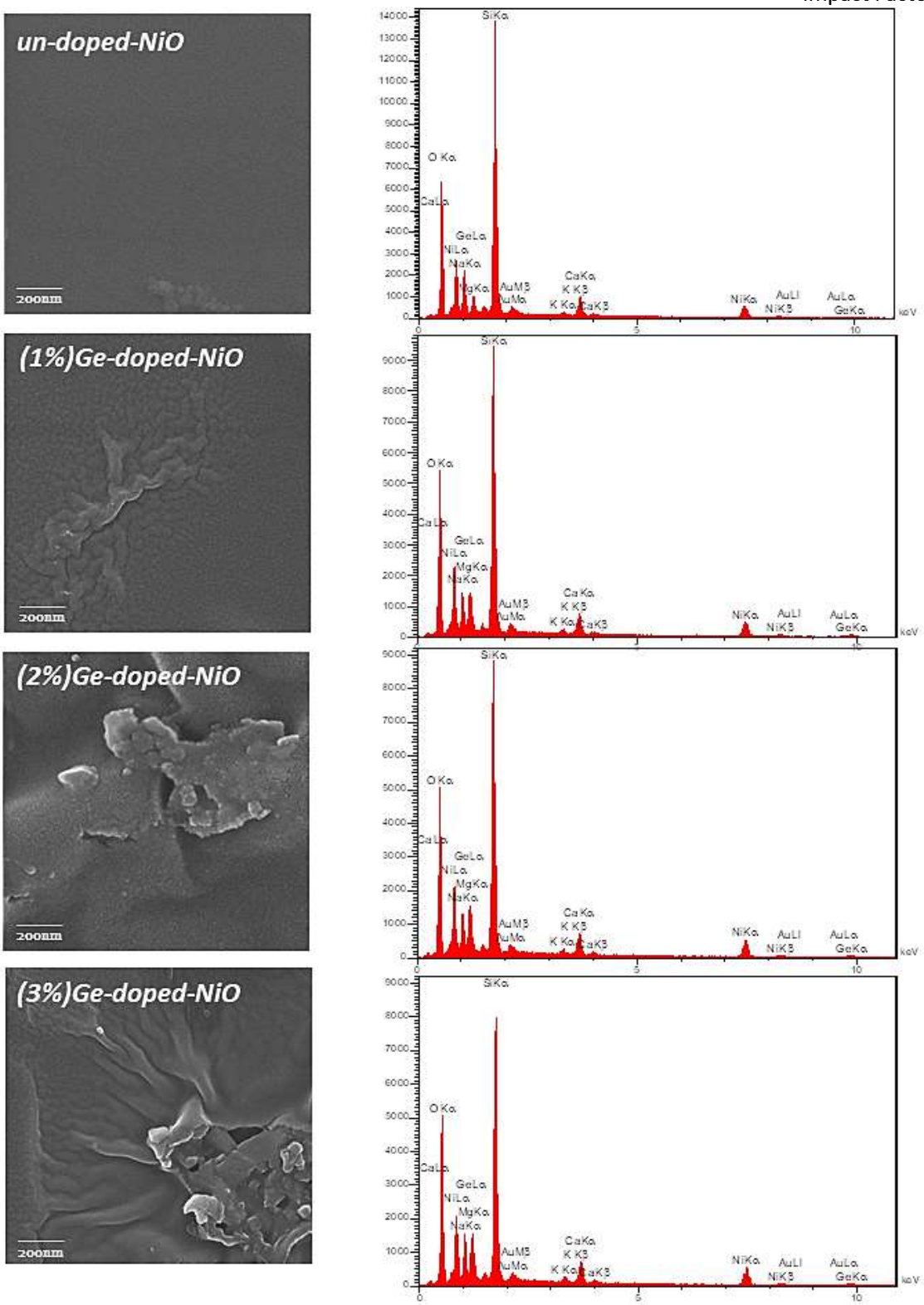

Fig.3: SEM and EDX characteristics for the NiO-based thin films with and without adding Ge at different concentrations

Un-doped NiO thin film has shown smooth surface morphology; this smooth morphology has changed to rougher and grainier surface with grains appeared bigger than the un-doped NiO thin film. Moreover, the surface roughness has increased after doping NiO thin film with 3% Ge, clear big grains appeared on the surface topography which might result in changing the lattice constant of NiO structure as suggested by Artia and co-authors [19]. This change in the structure topographies is found to be beneficial for higher transmittance

properties [19]. Furthermore, SEM was carried out in order to evaluate the structure components using Energy-dispersive X-ray spectroscopy (EDX) analysis which was employed to estimate the oxidation magnitude and the Ge doping of NiO nanostructures(see Fig.3). Due to the high electron energy beam used in SEM characterization, it is clear that the films have demonstrated obvious damage in some places. EDX analysis for the un-doped NiO shows higher oxygen content, this suggests that Ni has higher oxidation rate during the preparation process. Upon incorporation of Ge dopant into the NiO thin films, the oxygen content has reduced and the Ge content has increased slightly with increasing the doping concentration. Therefore, due to the low percentage of Ge dopants, it can be suggested that the Ge dopants have sufficiently incorporated into the NiO lattice structure [26].

3.3 Structural properties:

The structural properties of the NiO-based thin films were analyzed by X-ray diffractometer (Philips EXPERT MPD), Cu Kα radiation (λ=1.54 Å), the results are presented in Fig.4. The un-doped based NiO filmhas demonstrated a sharp peak related to the (111) phase at 37° [27]. Upon doping NiO thin films with Ge, the latter peak has disappeared and another peak at around 42° related to the phase (200) [28] has been observed which is attributed to NiO. Moreover, a new peak at around 48° related to the phase (220) has been observed [29]; this peak has correlated to Ge.There was a tendency with increasing Ge contents is observed, the two peaks (200-NiO) and (220-Ge) have demonstrated different diffraction intensities. Higher doping concentration (3%Ge) has resulted in lower peak intensities which have been attributed to the change in the structure order and crystallinity [19, 26].

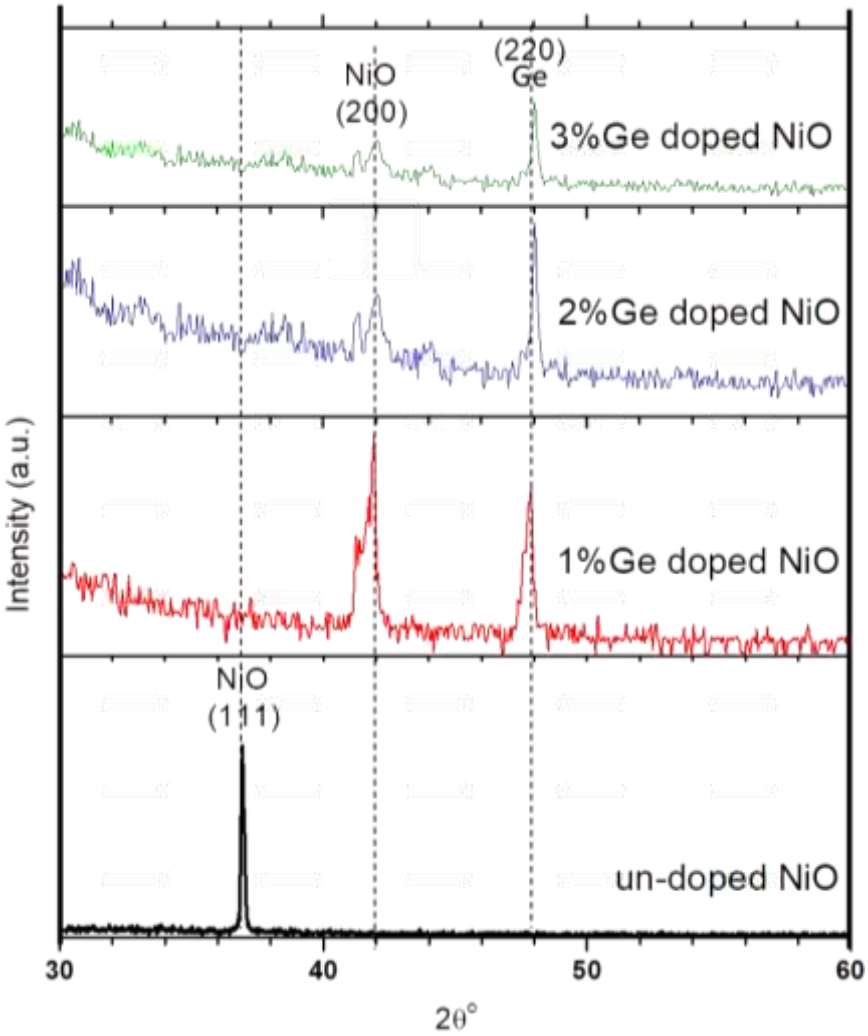

Fig.4: XRD patterns for the NiO-based thin films with and without adding Ge at different concentrations

3.4 Electrical conductivity and activation energy

The electrical conductivity (σ) of the NiO based thin filmshas been calculated by using the following equation [30]:

$$\sigma = \frac{1}{R}\frac{l}{w.t} \qquad (3)$$

where, R is the resistance of the thin film, w is the width, t is the film thickness, l is the distance between two (Al) poles. The conductivity of the un-doped NiO thin filmhasdecreased by increasing temperature, whereas the Ge-doped NiO have demonstrated totally different behavior;the electrical conductivity has increasedbydecreasing the temperature (see Fig.5a). This could be attributed to the increase in current with increasing temperature; heating causes more electrons to be freed (concentration of carriers increased) as they have more energy (from the thermal energy) to cross the band gap [31]. Furthermore, increasing the Ge content within NiO thin films has resulted in increasing the electrical conductivity; however, higher concentration of Ge (3%) has resulted in lower electrical conductivity which might be ascribed to the lattice constant change of NiO structure [19, 26].

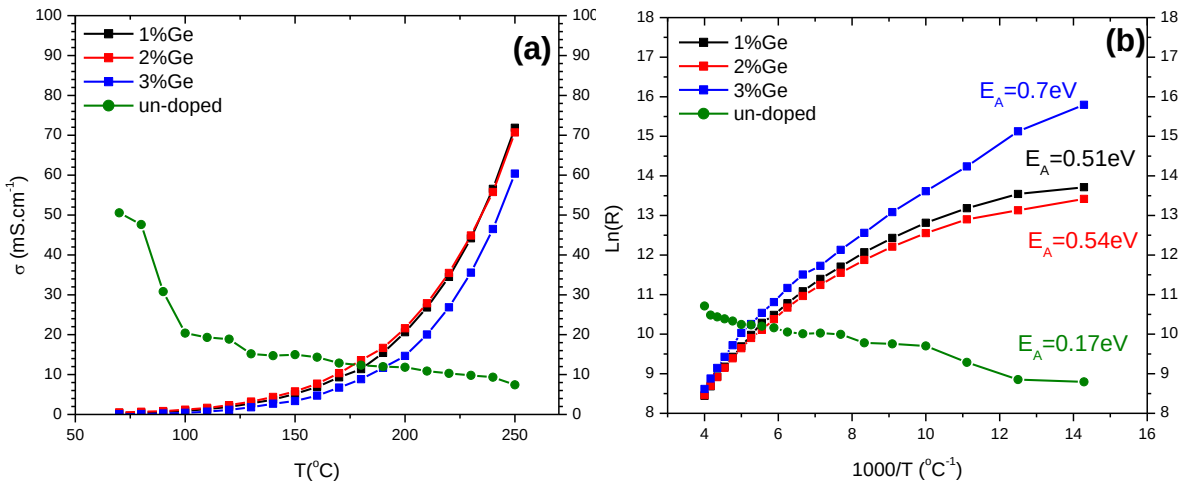

Fig.5: (a) Variation in the electrical conductivity with temperature and (b) Arrhenius plot of resistance for determination the activation energy, for NiO based thin films.

For the determination of the activation energy level (E_A) of un-doped and Ge-doped NiO thin films, the temperature dependence of dark electrical resistance has been measured and the data were fitted to Arrhenius equation [32]:

$$R = R_o \exp\left(\frac{E_A}{k_B T}\right) \qquad (4)$$

where R_o(is the pre-exponential factor [33]) is a parameter dependent on the sample characteristics (thickness, structure, etc.) and K_B is the Boltzmann constant. Fig.5b shows E_A of NiO based thin films which have increased from 0.28eV-0.6eVby doing with Ge and upon increasing temperature from 70°C -150°C. When temperature has increased from 150°C -250°C, E_A has shown an increase from 0.25eV to 1.17eV as illustrated in Table 1.

3.5 Seebeck coefficient:

In order to generate a temperature gradient along with the sample, two thermocouples at the ends ofthe sample were placed to record the generated temperature difference between the two ends of the sample.Afterward, a hot junction and a cold junctionwere created at each end.Generally, Seebeck effect is the impact of charge carrier diffusion where the charge carriers are pushed towards the cold side until voltage is built up. In case of ideal thermoelectric material, Seebeck coefficient should be large, produce large voltage and has low electrical resistivity to reduce Joule heating during operation, and low thermal conductivity to allow establishing temperature differences [34]. Seebeck effect could be defined by the following equation:

$$S = \frac{dV}{dT} \qquad (5)$$

A graph of the measured thermoelectric voltage versus temperature difference was plotted as shown in Fig.6. The slope of the curve gives the Seebeck coefficient of the thin film.The produced voltage as a function of

temperature for the un-doped NiO is found to increase exponentially with temperature; at transition temperatures (T_t) occur between 170°C-190°C (green highlighted in Fig.6), Seebeck coefficient has increased dramatically. Doping NiO with Ge has resulted in pulse-like voltage behavior with the same transition temperature (T_t) between 170-190°C (green highlighted in Fig.6). For this reason the temperatures below and above this range have been used to determine two different slops for two different regions. Seebeck coefficient of the un-doped NiO thin filmhas demonstrated positive value at both temperatures below and aboveT_t.This is evidence that NiO is a p-type semiconductor. Whereas, doping NiO with n-type dopant (Ge) has changing the semiconducting type to become n-type semiconductor, as indicated by the negative Seebeck coefficientfor both regions [35,36], see Table 1.

Table 1: The calculated parameters related to the NiO with and without doping by Ge

Thin film	E_g (eV)	E_A (eV)		Seebeck coefficient (S) ($\mu V.K^{-1}$)		
		Below T_t	Above T_t	Below T_t	Above T_t	Average
Un-doped NiO	3.65	0.28	0.25	0.2	42	-
1%Ge doped NiO	3.62	0.4	1.11	-3.6	-3	-3.3±(-0.3)
2%Ge doped NiO	3.62	0.36	1.02	-2.1	-2.5	-2.3±(-0.3)
3%Ge doped NiO	3.6	0.6	1.17	-3.1	-3	-3.05±(-0.05)

Usually, the negative Seebeck coefficient is indicated that the conduction band is slightly shifted toward Fermi level.This transition from p-type to n-type semiconductor has altered the density of states near the Fermi level, and removes the dependency of the unfavorable coupling between Seebeck coefficient and electrical conductivity [37]. As it has been mentioned before, the electrical conductivity has increased after doping with Ge, whereas Seebeck coefficient has shown more or less the same value for all the doping concentrations as shown in Table 1 (average value of Seebeck coefficient are illustrated in the Table 1).

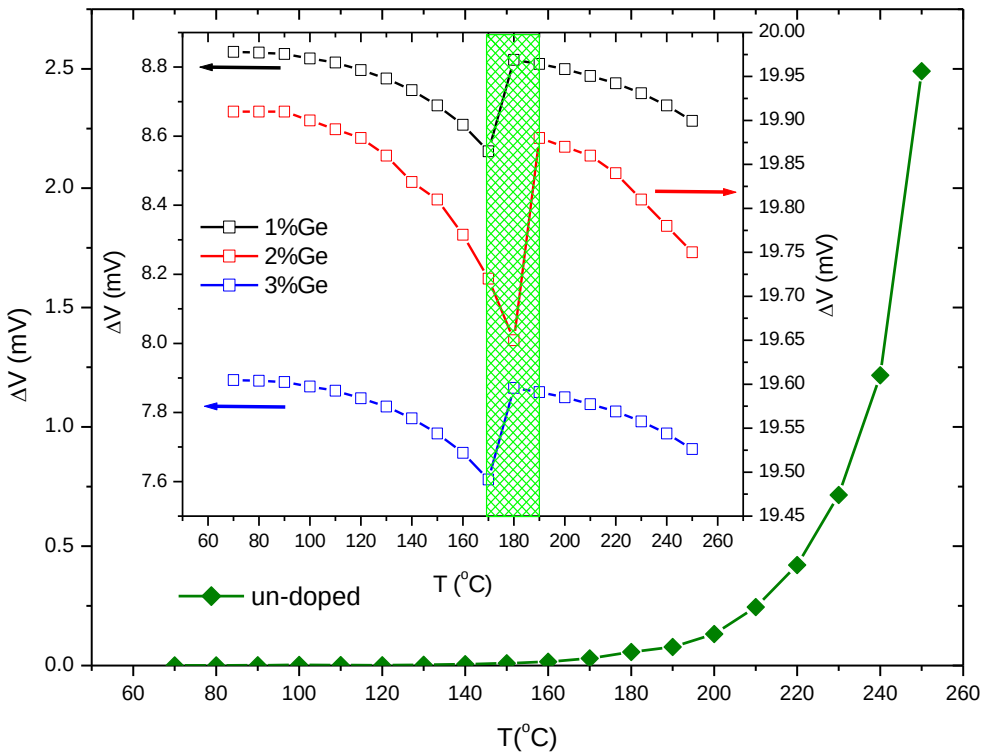

Fig.7: The variation of the Seebeck voltage versus the temperature difference across thesample

3.6 Power factor:

Power factor (PF) has been calculated using the following equation [38]:

$$PF = \sigma S^2 \quad (6)$$

As indicated by Seebeck coefficient results, no relation has been observed between electrical conductivity and Seebeck coefficient. Instead, PF has demonstrated an increase by increasing the Ge doping concentration as

shown in Fig.7. A slight increase in the PF for the un-doped NiO has been observed; while the 2%Ge-doped NiO has exhibited the highest obtained PF. This enhancement could be ascribed to the improved electrical conductivity. High power factor (PF) usually achieved by improving mobility, which is resulted from the variation in the carrier scattering mechanism [39]. On the other hand, the reduction in carrier mobility can deteriorate the electrical conductivity; therefore, increasing the electrical conductivity is the key factor to enhance PF [40, 41]. On the other hand, the coupled between Seebeck coefficient and electrical conductivity is via carrier concentration rather than charge carriers' mobility. Consequently, the improved mobility will increase the electrical conductivity without affecting the Seebeck coefficient, thus considerably improving the power factor [39].

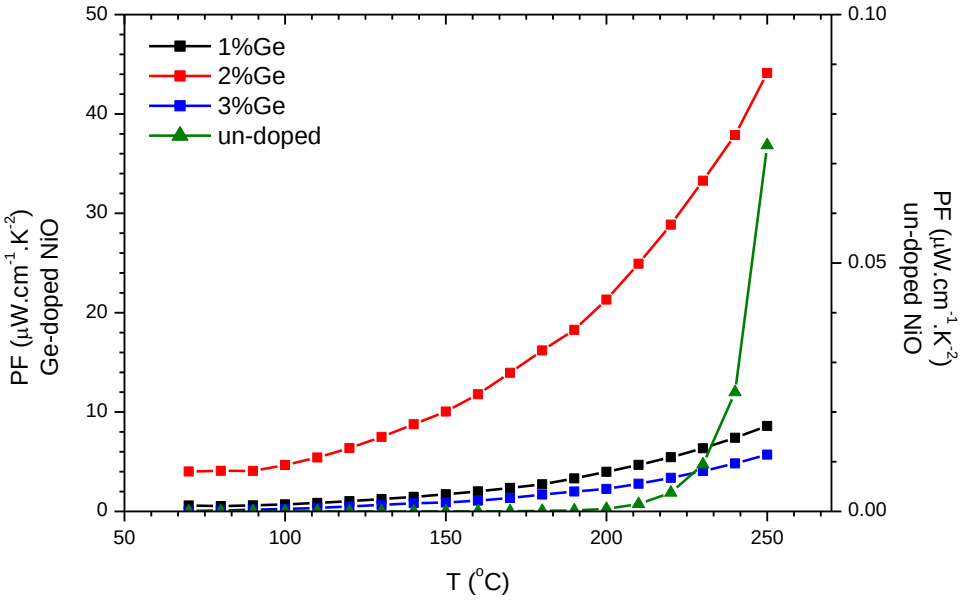

Fig.8: The variation of the power factor versus the temperature difference across the sample

CONCLUSION

NiO thin films have been investigated with and without doping with Ge by different concentration in order to use these layers in thermoelectric applications. The optical band gap has demonstrated a decrease after doping with Ge from 3.65eV (un-doped NiO thin film) to 3.6eV (3%Ge doped NiO thin film). The morphological features have shown rougher and grainier surface roughness after doping and have suggested a change in the structure. The latter has been confirmed by XRD with different phase appeared after doping and the XRD suggest that a change in lattice structure is occurred. The negative Seebeck coefficient has confirmed the transformation of NiO thin film from p-type semiconductor to n-type semiconductor. No relation between Seebeck coefficient and electrical conductivity has observed after doping and the increase the electrical conductivity without affecting the Seebeck coefficient, has resulted inimproving the power factor.

REFERENCES

[1] Dong, D., Wang, W., Barnabé, A., Presmanes, L., Rougier, A., Dong, G., Zhang, F., Yu, H., He, Y. and Diao, X., Enhanced electrochromism in short wavelengths for NiO:(Li, Mg) films in full inorganic device ITO/NiO:(Li, Mg)/Ta 2 O 5/WO 3/ITO. Electrochimica Acta, 263(2018):277-285.

[2] Zhou, D., Xie, D., Xia, X., Wang, X., Gu, C. and Tu, J., All-solid-state electrochromic devices based on WO 3|| NiO films: material developments and future applications. Science China Chemistry, 60(2017):3-12.

[3] Cabral, A.F., Remédios, C.M.R., Ospina, C.A., Carvalho, A.M.G. and Morelhão, S.L., Structure of antiferromagnetic NiO/ferrimagnetic NiMn2O4 composite prepared by sorbitol-assisted sol-gel method. Journal of Alloys and Compounds, 696(2017):304-309.

[4] Das, J. and Menon, K.S., On the evolution of antiferromagnetic nanodomains in NiO thin films: A LEEM study. Journal of Magnetism and Magnetic Materials, 449(2018):415-422.

[5] Zhou, Q., Umar, A., Amine, A., Xu, L., Gui, Y., Ibrahim, A.A., Kumar, R. and Baskoutas, S., Fabrication and characterization of highly sensitive and selective sensors based on porous NiO nanodisks. Sensors and Actuators B: Chemical, 259(2018):604-615.

[6] Gu, C., Cui, Y., Wang, L., Sheng, E., Shim, J.J. and Huang, J., Synthesis of the porous NiO/SnO2 microspheres and microcubes and their enhanced formaldehyde gas sensing performance. Sensors and Actuators B: Chemical, 241(2017):298-307.

[7] Chen, H.L., Lu, Y.M. and Hwang, W.S., Characterization of sputtered NiO thin films. Surface and Coatings Technology, 198(2005):138-142.

[8] Hasan, M.R., Xie, T., Barron, S.C., Liu, G., Nguyen, N.V., Motayed, A., Rao, M.V. and Debnath, R., Self-powered p-NiO/n-ZnO heterojunction ultraviolet photodetectors fabricated on plastic substrates. APL materials, 3(2015):106101.

[9] Koussi-Daoud, S., Pellegrin, Y., Odobel, F., Viana, B. and Pauporté, T., February. Electrodeposition of NiO films from various solvent electrolytic solutions for dye sensitized solar cell application. In Oxide-based Materials and Devices VIII 10105(2017):1010526. International Society for Optics and Photonics.

[10] Hammond, S.R., Olson, D.C. and Van Hest, M.F.A.M., SOLARWINDOW TECHNOLOGIES Inc and Alliance for Sustainable Energy LLC, Methods for producing thin film charge selective transport layers. U.S. Patent 9,859,515 (2018).

[11] Sun, H., Chen, S.C., Hsu, S.W., Wen, C.K., Chuang, T.H. and Wang, X., Microstructures and optoelectronic properties of nickel oxide films deposited by reactive magnetron sputtering at various working pressures of pure oxygen environment. Ceramics International, 43(2017):S369-S375.

[12] Singh, A., Bhansali, S., Barton, D. and Urban III, F.K., Reactive sputter deposition and annealing of nanometer scale NiO thin films for metal-insulator-metal tunnel junction diodes. Thin Solid Films, 644(2017):23-28.

[13] Turgut, E., Çoban, Ö., Sarıtaş, S., Tüzemen, S., Yıldırım, M. and Gür, E., Oxygen partial pressure effects on the RF sputtered p-type NiO hydrogen gas sensors. Applied Surface Science, 435(2018):880-885.

[14] Korotcenkov, G., Brinzari, V. and Ham, M.H., In2O3-Based Thermoelectric Materials: The State of the Art and the Role of Surface State in the Improvement of the Efficiency of Thermoelectric Conversion. Crystals, 8(2018):14.

[15] Budak, S., Gulduren, E., Allen, B., Cole, J., Lassiter, J., Colon, T., Muntele, C., Parker, R., Smith, C. and Johnson, R.B., High Energy Radiation Effects on the Seebeck Coefficient, van der Pauw-Hall Effect Parameters and Optical Properties of Si/Si+ Sb Multi-Nanolayered Thin Films. American Journal of Materials Science, 5(2015):39-47.

[16] Lee, H.J., Park, H.S., Han, S. and Kim, J.Y., Thermoelectric properties of n-type Bi–Te thin films with deposition conditions using RF magnetron co-sputtering. Thermochimica acta, 542(2012):57-61.

[17] Ping Fan, Ying-zhen Li, Zhuang-hao Zheng, Qing-yun Lin, Jing-ting Luo, Guang-xing Liang, Miao-qin Zhang, Min-cong Chen, "Thermoelectric properties optimization of Al-doped ZnO thin films prepared by reactive sputtering Zn–Al alloy target", Applied Surface Science 284(2013):145-149.

[18] Mao, J., Shuai, J., Song, S., Wu, Y., Dally, R., Zhou, J., Liu, Z., Sun, J., Zhang, Q., dela Cruz, C. and Wilson, S., Manipulation of ionized impurity scattering for achieving high thermoelectric performance in n-type Mg3Sb2-based materials. Proceedings of the National Academy of Sciences, (2017):201711725.

[19] Arita, M., Yamaguchi, M. and Masuda, M., Electrical and optical properties of germanium-doped zinc oxide thin films. Materials transactions, 45(2004):3180-3183.

[20] Ryu H.Y., Choi G.P., Lee W.S., Park J.S., Preferred orientations of NiO thin films prepared by RF magnetron sputtering, Journal of Materials Science 39(2004):4375-4377.

[21] Li, H.K., Chen, T.P., Hu, S.G., Li, X.D., Liu, Y., Lee, P.S., Wang, X.P., Li, H.Y. and Lo, G.Q., Highly spectrum-selective ultraviolet photodetector based on p-NiO/n-IGZO thin film heterojunction structure. Optics express, 23(2015):27683-27689.

[22] Lu, Yang-Ming, Weng-Sing Hwang, J. S. Yang, and H. C. Chuang. "Properties of nickel oxide thin films deposited by RF reactive magnetron sputtering." Thin Solid Films 420 (2002):54-61.

[23] Y. Wang, L. Zhang, K. Deng, X. Chen, Z. Zou, Low temperature synthesis and photocatalytic activity of rutile TiO2 nanorod superstructures. J. Phys. Chem. C. 111(2007):2709-2714.

[24] P.K.K. Kumarasinghe, A. Dissanayake, B.M.K. Pemasiri, B.S. Dassanayake, Thermally evaporated CdTe thin films for solar cell applications: Optimization of physical properties. Mater. Res. Bull. 96(2017):188–195.

[25] Al-hashimi, Mohammed K., Burak Y. Kadem, and Aseel K. Hassan. "Rutile TiO2 films as electron transport layer in inverted organic solar cell." Journal of Materials Science: Materials in Electronics (2018): 1-9.

[26] Allaedini, G., Aminayi, P. and Tasirin, S.M., Structural properties and optical characterization of flower-like Mg doped NiO. AIP Advances, 5(2015):077161.

[27] Zhai, P., Yi, Q., Jian, J., Wang, H., Song, P., Dong, C., Lu, X., Sun, Y., Zhao, J., Dai, X. and Lou, Y.,Transparent p-type epitaxial thin films of nickel oxide. Chemical Communications, 50(2014):1854-1856.
[28] Irwin, M.D., Buchholz, D.B., Hains, A.W., Chang, R.P. and Marks, T.J., p-Type semiconducting nickel oxide as an efficiency-enhancing anode interfacial layer in polymer bulk-heterojunction solar cells. Proceedings of the National Academy of Sciences, 105(2008):2783-2787.
[29] Choe, H.S., Kim, S.J., Kim, M.C., Kim, D.M., Lee, G.H., Han, S.B., Kwak, D.H. and Park, K.W., Synthesis of Ge/C composites as anodes using glucose as a reductant and carbon source for lithium-ion batteries. RSC Advances, 6(2016):72926-72932.
[30] Kadem, B., Cranton, W. and Hassan, A., Metal salt modified PEDOT: PSS as anode buffer layer and its effect on power conversion efficiency of organic solar cells. Organic Electronics, 24(2015):73-79.
[31] Hassan, A.J., Study of optical and electrical properties of nickel oxide (NiO) thin films deposited by using a spray pyrolysis technique. Journal of Modern Physics, 5(2014):2184.
[32] Guneri, E., Ulutas, C., Kirmizigul, F., Altindemir, G., Gode, F. and Gumus, C., Effect of deposition time on structural, electrical, and optical properties of SnS thin films deposited by chemical bath deposition. applied surface science, 257(2010):1189-1195.
[33] Batal, M.A., Nashed, G. and Jneed, F.H., Conductivity and thermoelectric properties of nanostructure tin oxide thin films. Journal of the Association of Arab Universities for Basic and Applied Sciences, 15(2014):15-20.
[34] Noori, A., Masoumi, S. and Hashemi, N., December. Temperature Dependence of the Seebeck Coefficient in Zinc Oxide Thin Films. In Journal of Physics: Conference Series, 939(2017):012013. IOP Publishing.
[35] Sun, P., Wei, B., Zhang, J., Tomczak, J.M., Strydom, A.M., Søndergaard, M., Iversen, B.B. and Steglich, F.,Large Seebeck effect by charge-mobility engineering. Nature communications, 6(2015):7475.
[36] Nonoguchi, Y., Ohashi, K., Kanazawa, R., Ashiba, K., Hata, K., Nakagawa, T., Adachi, C., Tanase, T. and Kawai, T., Systematic conversion of single walled carbon nanotubes into n-type thermoelectric materials by molecular dopants. Scientific reports, 3(2013):3344.
[37] Gaul, A., Peng, Q., Singh, D.J., Ramanath, G. and Borca-Tasciuc, T., Pressure-induced insulator-to-metal transitions for enhancing thermoelectric power factor in bismuth telluride-based alloys. Physical Chemistry Chemical Physics, 19(2017):12784-12793.
[38] Qusiy H. Al-Galiby, Hatef Sadeghi, David Zsolt Manrique and Colin J. Lambert, Tuning the Seebeck coefficient of naphthalenediimide by electrochemical gating and doping, Nanoscale, 9(2017):4819.
[39] Mao, J., Shuai, J., Song, S., Wu, Y., Dally, R., Zhou, J., Liu, Z., Sun, J., Zhang, Q., dela Cruz, C. and Wilson, S., Manipulation of ionized impurity scattering for achieving high thermoelectric performance in n-type Mg3Sb2-based materials. Proceedings of the National Academy of Sciences, (2017):201711725.
[40] Heremans, J.P., Jovovic, V., Toberer, E.S., Saramat, A., Kurosaki, K., Charoenphakdee, A., Yamanaka, S. and Snyder, G.J., Enhancement of thermoelectric efficiency in PbTe by distortion of the electronic density of states. Science, 321(2008):554-557.
[41] Wang, S., Yang, J., Wu, L., Wei, P., Zhang, W. and Yang, J., On Intensifying carrier impurity scattering to enhance thermoelectric performance in Cr-doped CeyCo4Sb12. Advanced Functional Materials, 25(2015):6660-6670.